BABAR-PUB-03/001
SLAC-PUB-9644

Measurement of $B^0 \to D_s^{(*)+} D^{*-}$ Branching Fractions and $B^0 \to D_s^{*+} D^{*-}$ Polarization with a Partial Reconstruction Technique

B. Aubert,[1] R. Barate,[1] D. Boutigny,[1] J.-M. Gaillard,[1] A. Hicheur,[1] Y. Karyotakis,[1] J. P. Lees,[1] P. Robbe,[1] V. Tisserand,[1] A. Zghiche,[1] A. Palano,[2] A. Pompili,[2] J. C. Chen,[3] N. D. Qi,[3] G. Rong,[3] P. Wang,[3] Y. S. Zhu,[3] G. Eigen,[4] I. Ofte,[4] B. Stugu,[4] G. S. Abrams,[5] A. W. Borgland,[5] A. B. Breon,[5] D. N. Brown,[5] J. Button-Shafer,[5] R. N. Cahn,[5] E. Charles,[5] M. S. Gill,[5] A. V. Gritsan,[5] Y. Groysman,[5] R. G. Jacobsen,[5] R. W. Kadel,[5] J. Kadyk,[5] L. T. Kerth,[5] Yu. G. Kolomensky,[5] J. F. Kral,[5] C. LeClerc,[5] M. E. Levi,[5] G. Lynch,[5] L. M. Mir,[5] P. J. Oddone,[5] T. J. Orimoto,[5] M. Pripstein,[5] N. A. Roe,[5] A. Romosan,[5] M. T. Ronan,[5] V. G. Shelkov,[5] A. V. Telnov,[5] W. A. Wenzel,[5] T. J. Harrison,[6] C. M. Hawkes,[6] D. J. Knowles,[6] S. W. O'Neale,[6] R. C. Penny,[6] A. T. Watson,[6] N. K. Watson,[6] T. Deppermann,[7] K. Goetzen,[7] H. Koch,[7] B. Lewandowski,[7] M. Pelizaeus,[7] K. Peters,[7] H. Schmuecker,[7] M. Steinke,[7] N. R. Barlow,[8] W. Bhimji,[8] J. T. Boyd,[8] N. Chevalier,[8] P. J. Clark,[8] W. N. Cottingham,[8] C. Mackay,[8] F. F. Wilson,[8] C. Hearty,[9] T. S. Mattison,[9] J. A. McKenna,[9] D. Thiessen,[9] S. Jolly,[10] P. Kyberd,[10] A. K. McKemey,[10] V. E. Blinov,[11] A. D. Bukin,[11] V. B. Golubev,[11] V. N. Ivanchenko,[11] E. A. Kravchenko,[11] A. P. Onuchin,[11] S. I. Serednyakov,[11] Yu. I. Skovpen,[11] A. N. Yushkov,[11] D. Best,[12] M. Chao,[12] D. Kirkby,[12] A. J. Lankford,[12] M. Mandelkern,[12] S. McMahon,[12] R. K. Mommsen,[12] W. Roethel,[12] D. P. Stoker,[12] K. Arisaka,[13] C. Buchanan,[13] H. K. Hadavand,[14] E. J. Hill,[14] D. B. MacFarlane,[14] H. P. Paar,[14] Sh. Rahatlou,[14] G. Raven,[14] U. Schwanke,[14] V. Sharma,[14] J. W. Berryhill,[15] C. Campagnari,[15] B. Dahmes,[15] N. Kuznetsova,[15] S. L. Levy,[15] O. Long,[15] A. Lu,[15] M. A. Mazur,[15] J. D. Richman,[15] W. Verkerke,[15] J. Beringer,[16] A. M. Eisner,[16] C. A. Heusch,[16] W. S. Lockman,[16] T. Schalk,[16] R. E. Schmitz,[16] B. A. Schumm,[16] A. Seiden,[16] M. Turri,[16] W. Walkowiak,[16] D. C. Williams,[16] M. G. Wilson,[16] J. Albert,[17] E. Chen,[17] G. P. Dubois-Felsmann,[17] A. Dvoretskii,[17] D. G. Hitlin,[17] I. Narsky,[17] F. C. Porter,[17] A. Ryd,[17] A. Samuel,[17] S. Yang,[17] S. Jayatilleke,[18] G. Mancinelli,[18] B. T. Meadows,[18] M. D. Sokoloff,[18] T. Barillari,[19] F. Blanc,[19] P. Bloom,[19] W. T. Ford,[19] U. Nauenberg,[19] A. Olivas,[19] P. Rankin,[19] J. Roy,[19] J. G. Smith,[19] W. C. van Hoek,[19] L. Zhang,[19] J. L. Harton,[20] T. Hu,[20] A. Soffer,[20] W. H. Toki,[20] R. J. Wilson,[20] J. Zhang,[20] D. Altenburg,[21] T. Brandt,[21] J. Brose,[21] T. Colberg,[21] M. Dickopp,[21] R. S. Dubitzky,[21] A. Hauke,[21] H. M. Lacker,[21] E. Maly,[21] R. Müller-Pfefferkorn,[21] R. Nogowski,[21] S. Otto,[21] K. R. Schubert,[21] R. Schwierz,[21] B. Spaan,[21] L. Wilden,[21] D. Bernard,[22] G. R. Bonneaud,[22] F. Brochard,[22] J. Cohen-Tanugi,[22] S. T'Jampens,[22] Ch. Thiebaux,[22] G. Vasileiadis,[22] M. Verderi,[22] A. Anjomshoaa,[23] R. Bernet,[23] A. Khan,[23] D. Lavin,[23] F. Muheim,[23] S. Playfer,[23] J. E. Swain,[23] J. Tinslay,[23] C. Borean,[24] C. Bozzi,[24] L. Piemontese,[24] A. Sarti,[24] E. Treadwell,[25] F. Anulli,[26,*] R. Baldini-Ferroli,[26] A. Calcaterra,[26] R. de Sangro,[26] D. Falciai,[26] G. Finocchiaro,[26] P. Patteri,[26] I. M. Peruzzi,[26,*] M. Piccolo,[26] A. Zallo,[26] S. Bagnasco,[27] A. Buzzo,[27] R. Contri,[27] G. Crosetti,[27] M. Lo Vetere,[27] M. Macri,[27] M. R. Monge,[27] S. Passaggio,[27] F. C. Pastore,[27] C. Patrignani,[27] E. Robutti,[27] A. Santroni,[27] S. Tosi,[27] S. Bailey,[28] M. Morii,[28] G. J. Grenier,[29] S.-J. Lee,[29] U. Mallik,[29] J. Cochran,[30] H. B. Crawley,[30] J. Lamsa,[30] W. T. Meyer,[30] S. Prell,[30] E. I. Rosenberg,[30] J. Yi,[30] M. Davier,[31] G. Grosdidier,[31] A. Höcker,[31] S. Laplace,[31] F. Le Diberder,[31] V. Lepeltier,[31] A. M. Lutz,[31] T. C. Petersen,[31] S. Plaszczynski,[31] M. H. Schune,[31] L. Tantot,[31] G. Wormser,[31] R. M. Bionta,[32] V. Brigljević,[32] C. H. Cheng,[32] D. J. Lange,[32] K. van Bibber,[32] D. M. Wright,[32] A. J. Bevan,[33] J. R. Fry,[33] E. Gabathuler,[33] R. Gamet,[33] M. Kay,[33] D. J. Payne,[33] R. J. Sloane,[33] C. Touramanis,[33] M. L. Aspinwall,[34] D. A. Bowerman,[34] P. D. Dauncey,[34] U. Egede,[34] I. Eschrich,[34] G. W. Morton,[34] J. A. Nash,[34] P. Sanders,[34] G. P. Taylor,[34] J. J. Back,[35] G. Bellodi,[35] P. Dixon,[35] P. F. Harrison,[35] H. W. Shorthouse,[35] P. Strother,[35] P. B. Vidal,[35] G. Cowan,[36] H. U. Flaecher,[36] S. George,[36] M. G. Green,[36] A. Kurup,[36] C. E. Marker,[36] T. R. McMahon,[36] S. Ricciardi,[36] F. Salvatore,[36] G. Vaitsas,[36] M. A. Winter,[36] D. Brown,[37] C. L. Davis,[37] J. Allison,[38] R. J. Barlow,[38] A. C. Forti,[38] P. A. Hart,[38] F. Jackson,[38] G. D. Lafferty,[38] A. J. Lyon,[38] J. H. Weatherall,[38] J. C. Williams,[38] A. Farbin,[39] A. Jawahery,[39] V. Lillard,[39] D. A. Roberts,[39] G. Blaylock,[40] C. Dallapiccola,[40] K. T. Flood,[40] S. S. Hertzbach,[40] R. Kofler,[40] V. B. Koptchev,[40] T. B. Moore,[40] H. Staengle,[40] S. Willocq,[40] R. Cowan,[41] G. Sciolla,[41] F. Taylor,[41] R. K. Yamamoto,[41] D. J. J. Mangeol,[42] M. Milek,[42] P. M. Patel,[42] F. Palombo,[43] J. M. Bauer,[44] L. Cremaldi,[44] V. Eschenburg,[44] R. Kroeger,[44] J. Reidy,[44] D. A. Sanders,[44] D. J. Summers,[44] H. W. Zhao,[44] C. Hast,[45] P. Taras,[45] H. Nicholson,[46] C. Cartaro,[47] N. Cavallo,[47] G. De Nardo,[47] F. Fabozzi,[47,†] C. Gatto,[47] L. Lista,[47] P. Paolucci,[47] D. Piccolo,[47] C. Sciacca,[47] J. M. LoSecco,[48] T. A. Gabriel,[49] B. Brau,[50] T. Pulliam,[50] J. Brau,[51] R. Frey,[51] M. Iwasaki,[51] C. T. Potter,[51]

N. B. Sinev,[51] D. Strom,[51] E. Torrence,[51] F. Colecchia,[52] A. Dorigo,[52] F. Galeazzi,[52] M. Margoni,[52] M. Morandin,[52] M. Posocco,[52] M. Rotondo,[52] F. Simonetto,[52] R. Stroili,[52] G. Tiozzo,[52] C. Voci,[52] M. Benayoun,[53] H. Briand,[53] J. Chauveau,[53] P. David,[53] Ch. de la Vaissière,[53] L. Del Buono,[53] O. Hamon,[53] Ph. Leruste,[53] J. Ocariz,[53] M. Pivk,[53] L. Roos,[53] J. Stark,[53] P. F. Manfredi,[54] V. Re,[54] V. Speziali,[54] L. Gladney,[55] Q. H. Guo,[55] J. Panetta,[55] C. Angelini,[56] G. Batignani,[56] S. Bettarini,[56] M. Bondioli,[56] F. Bucci,[56] G. Calderini,[56] E. Campagna,[56] M. Carpinelli,[56] F. Forti,[56] M. A. Giorgi,[56] A. Lusiani,[56] G. Marchiori,[56] F. Martinez-Vidal,[56] M. Morganti,[56] N. Neri,[56] E. Paoloni,[56] M. Rama,[56] G. Rizzo,[56] F. Sandrelli,[56] G. Triggiani,[56] J. Walsh,[56] M. Haire,[57] D. Judd,[57] K. Paick,[57] D. E. Wagoner,[57] N. Danielson,[58] P. Elmer,[58] C. Lu,[58] V. Miftakov,[58] J. Olsen,[58] A. J. S. Smith,[58] A. Tumanov,[58] E. W. Varnes,[58] F. Bellini,[59] G. Cavoto,[58,59] D. del Re,[59] R. Faccini,[14,59] F. Ferrarotto,[59] F. Ferroni,[59] M. Gaspero,[59] E. Leonardi,[59] M. A. Mazzoni,[59] S. Morganti,[59] M. Pierini,[59] G. Piredda,[59] F. Safai Tehrani,[59] M. Serra,[59] C. Voena,[59] S. Christ,[60] G. Wagner,[60] R. Waldi,[60] T. Adye,[61] N. De Groot,[61] B. Franek,[61] N. I. Geddes,[61] G. P. Gopal,[61] E. O. Olaiya,[61] S. M. Xella,[61] R. Aleksan,[62] S. Emery,[62] A. Gaidot,[62] S. F. Ganzhur,[62] P.-F. Giraud,[62] G. Hamel de Monchenault,[62] W. Kozanecki,[62] M. Langer,[62] G. W. London,[62] B. Mayer,[62] G. Schott,[62] B. Serfass,[62] G. Vasseur,[62] Ch. Yeche,[62] M. Zito,[62] M. V. Purohit,[63] A. W. Weidemann,[63] F. X. Yumiceva,[63] K. Abe,[64] D. Aston,[64] R. Bartoldus,[64] N. Berger,[64] A. M. Boyarski,[64] O. L. Buchmueller,[64] M. R. Convery,[64] D. P. Coupal,[64] D. Dong,[64] J. Dorfan,[64] W. Dunwoodie,[64] R. C. Field,[64] T. Glanzman,[64] S. J. Gowdy,[64] E. Grauges-Pous,[64] T. Hadig,[64] V. Halyo,[64] T. Himel,[64] T. Hryn'ova,[64] W. R. Innes,[64] C. P. Jessop,[64] M. H. Kelsey,[64] P. Kim,[64] M. L. Kocian,[64] U. Langenegger,[64] D. W. G. S. Leith,[64] S. Luitz,[64] V. Luth,[64] H. L. Lynch,[64] H. Marsiske,[64] S. Menke,[64] R. Messner,[64] D. R. Muller,[64] C. P. O'Grady,[64] V. E. Ozcan,[64] A. Perazzo,[64] M. Perl,[64] S. Petrak,[64] B. N. Ratcliff,[64] S. H. Robertson,[64] A. Roodman,[64] A. A. Salnikov,[64] T. Schietinger,[64] R. H. Schindler,[64] J. Schwiening,[64] G. Simi,[64] A. Snyder,[64] A. Soha,[64] J. Stelzer,[64] D. Su,[64] M. K. Sullivan,[64] H. A. Tanaka,[64] J. Va'vra,[64] S. R. Wagner,[64] M. Weaver,[64] A. J. R. Weinstein,[64] W. J. Wisniewski,[64] D. H. Wright,[64] C. C. Young,[64] P. R. Burchat,[65] T. I. Meyer,[65] C. Roat,[65] W. Bugg,[66] M. Krishnamurthy,[66] S. M. Spanier,[66] J. M. Izen,[67] I. Kitayama,[67] X. C. Lou,[67] F. Bianchi,[68] M. Bona,[68] D. Gamba,[68] L. Bosisio,[69] G. Della Ricca,[69] S. Dittongo,[69] L. Lanceri,[69] P. Poropat,[69] L. Vitale,[69] G. Vuagnin,[69] R. Henderson,[70] R. S. Panvini,[71] Sw. Banerjee,[72] C. M. Brown,[72] D. Fortin,[72] P. D. Jackson,[72] R. Kowalewski,[72] J. M. Roney,[72] H. R. Band,[73] S. Dasu,[73] M. Datta,[73] A. M. Eichenbaum,[73] H. Hu,[73] J. R. Johnson,[73] R. Liu,[73] F. Di Lodovico,[73] A. K. Mohapatra,[73] Y. Pan,[73] R. Prepost,[73] S. J. Sekula,[73] J. H. von Wimmersperg-Toeller,[73] J. Wu,[73] S. L. Wu,[73] Z. Yu,[73] and H. Neal[74]

(The *BABAR* Collaboration)

[1]*Laboratoire de Physique des Particules, F-74941 Annecy-le-Vieux, France*
[2]*Università di Bari, Dipartimento di Fisica and INFN, I-70126 Bari, Italy*
[3]*Institute of High Energy Physics, Beijing 100039, China*
[4]*University of Bergen, Inst. of Physics, N-5007 Bergen, Norway*
[5]*Lawrence Berkeley National Laboratory and University of California, Berkeley, CA 94720, USA*
[6]*University of Birmingham, Birmingham, B15 2TT, United Kingdom*
[7]*Ruhr Universität Bochum, Institut für Experimentalphysik 1, D-44780 Bochum, Germany*
[8]*University of Bristol, Bristol BS8 1TL, United Kingdom*
[9]*University of British Columbia, Vancouver, BC, Canada V6T 1Z1*
[10]*Brunel University, Uxbridge, Middlesex UB8 3PH, United Kingdom*
[11]*Budker Institute of Nuclear Physics, Novosibirsk 630090, Russia*
[12]*University of California at Irvine, Irvine, CA 92697, USA*
[13]*University of California at Los Angeles, Los Angeles, CA 90024, USA*
[14]*University of California at San Diego, La Jolla, CA 92093, USA*
[15]*University of California at Santa Barbara, Santa Barbara, CA 93106, USA*
[16]*University of California at Santa Cruz, Institute for Particle Physics, Santa Cruz, CA 95064, USA*
[17]*California Institute of Technology, Pasadena, CA 91125, USA*
[18]*University of Cincinnati, Cincinnati, OH 45221, USA*
[19]*University of Colorado, Boulder, CO 80309, USA*
[20]*Colorado State University, Fort Collins, CO 80523, USA*
[21]*Technische Universität Dresden, Institut für Kern- und Teilchenphysik, D-01062 Dresden, Germany*
[22]*Ecole Polytechnique, LLR, F-91128 Palaiseau, France*
[23]*University of Edinburgh, Edinburgh EH9 3JZ, United Kingdom*
[24]*Università di Ferrara, Dipartimento di Fisica and INFN, I-44100 Ferrara, Italy*
[25]*Florida A&M University, Tallahassee, FL 32307, USA*
[26]*Laboratori Nazionali di Frascati dell'INFN, I-00044 Frascati, Italy*
[27]*Università di Genova, Dipartimento di Fisica and INFN, I-16146 Genova, Italy*
[28]*Harvard University, Cambridge, MA 02138, USA*

[29]University of Iowa, Iowa City, IA 52242, USA
[30]Iowa State University, Ames, IA 50011-3160, USA
[31]Laboratoire de l'Accélérateur Linéaire, F-91898 Orsay, France
[32]Lawrence Livermore National Laboratory, Livermore, CA 94550, USA
[33]University of Liverpool, Liverpool L69 3BX, United Kingdom
[34]University of London, Imperial College, London, SW7 2BW, United Kingdom
[35]Queen Mary, University of London, E1 4NS, United Kingdom
[36]University of London, Royal Holloway and Bedford New College, Egham, Surrey TW20 0EX, United Kingdom
[37]University of Louisville, Louisville, KY 40292, USA
[38]University of Manchester, Manchester M13 9PL, United Kingdom
[39]University of Maryland, College Park, MD 20742, USA
[40]University of Massachusetts, Amherst, MA 01003, USA
[41]Massachusetts Institute of Technology, Laboratory for Nuclear Science, Cambridge, MA 02139, USA
[42]McGill University, Montréal, QC, Canada H3A 2T8
[43]Università di Milano, Dipartimento di Fisica and INFN, I-20133 Milano, Italy
[44]University of Mississippi, University, MS 38677, USA
[45]Université de Montréal, Laboratoire René J. A. Lévesque, Montréal, QC, Canada H3C 3J7
[46]Mount Holyoke College, South Hadley, MA 01075, USA
[47]Università di Napoli Federico II, Dipartimento di Scienze Fisiche and INFN, I-80126, Napoli, Italy
[48]University of Notre Dame, Notre Dame, IN 46556, USA
[49]Oak Ridge National Laboratory, Oak Ridge, TN 37831, USA
[50]Ohio State University, Columbus, OH 43210, USA
[51]University of Oregon, Eugene, OR 97403, USA
[52]Università di Padova, Dipartimento di Fisica and INFN, I-35131 Padova, Italy
[53]Universités Paris VI et VII, Lab de Physique Nucléaire H. E., F-75252 Paris, France
[54]Università di Pavia, Dipartimento di Elettronica and INFN, I-27100 Pavia, Italy
[55]University of Pennsylvania, Philadelphia, PA 19104, USA
[56]Università di Pisa, Dipartimento di fisica, Scuola Normale Superiore and INFN, I-56010 Pisa, Italy
[57]Prairie View A&M University, Prairie View, TX 77446, USA
[58]Princeton University, Princeton, NJ 08544, USA
[59]Università di Roma La Sapienza, Dipartimento di Fisica and INFN, I-00185 Roma, Italy
[60]Universität Rostock, D-18051 Rostock, Germany
[61]Rutherford Appleton Laboratory, Chilton, Didcot, Oxon, OX11 0QX, United Kingdom
[62]DAPNIA, Commissariat à l'Energie Atomique/Saclay, F-91191 Gif-sur-Yvette, France
[63]University of South Carolina, Columbia, SC 29208, USA
[64]Stanford Linear Accelerator Center, Stanford, CA 94309, USA
[65]Stanford University, Stanford, CA 94305-4060, USA
[66]University of Tennessee, Knoxville, TN 37996, USA
[67]University of Texas at Dallas, Richardson, TX 75083, USA
[68]Università di Torino, Dipartimento di Fisica Sperimentale and INFN, I-10125 Torino, Italy
[69]Università di Trieste, Dipartimento di Fisica and INFN, I-34127 Trieste, Italy
[70]TRIUMF, Vancouver, BC, Canada V6T 2A3
[71]Vanderbilt University, Nashville, TN 37235, USA
[72]University of Victoria, Victoria, BC, Canada V8W 3P6
[73]University of Wisconsin, Madison, WI 53706, USA
[74]Yale University, New Haven, CT 06511, USA

(Dated: September 30, 2017)

We present a study of the decays $B^0 \to D_s^{(*)+} D^{*-}$, using $20.8\,\mathrm{fb}^{-1}$ of e^+e^- annihilation data recorded with the *BABAR* detector. The analysis is conducted with a partial reconstruction technique, in which only the $D_s^{(*)+}$ and the soft pion from the D^{*-} decay are reconstructed. We measure the branching fractions $\mathcal{B}(B^0 \to D_s^+ D^{*-}) = (1.03 \pm 0.14 \pm 0.13 \pm 0.26)\%$ and $\mathcal{B}(B^0 \to D_s^{*+} D^{*-}) = (1.97 \pm 0.15 \pm 0.30 \pm 0.49)\%$, where the first error is statistical, the second is systematic, and the third is the error due to the $D_s^+ \to \phi\pi^+$ branching fraction uncertainty. From the $B^0 \to D_s^{*+} D^{*-}$ angular distributions, we measure the fraction of longitudinal polarization $\Gamma_L/\Gamma = (51.9 \pm 5.0 \pm 2.8)\%$, which is consistent with theoretical predictions based on factorization.

PACS numbers: 13.25.Hw, 13.25.-k, 14.40.Nd

*Also with Università di Perugia, Perugia, Italy

†Also with Università della Basilicata, Potenza, Italy

I. INTRODUCTION

Precise knowledge of the branching fractions of exclusive B decay modes provides a test of the factorization approach [1]. Factorization neglects final state interactions between the quarks of the two final state mesons. The pattern of branching fractions for two-body B decays to modes such as $D^{(*)}\pi$, $D^{(*)}\rho$ [2] can be successfully accommodated in such a model. However, it is possible that the factorization assumption is not applicable to the decays $B \to D^{(*)}X$, where the meson X contains a heavy quark. The current experimental uncertainties for $B \to D_s^{(*)+}\overline{D}^*$ branching fractions [3] do not allow us to perform a precise test of the factorization approach in this case.

Further tests of factorization are provided by measuring the polarization in decays of B mesons to vector-vector final states. Within experimental errors, polarization measurements are consistent with factorization predictions for the final states $\overline{D}^*\rho$ [4], $\overline{D}^*\rho(1450)$ [5], and $D_s^*\overline{D}^*$ [6].

In this paper we present measurements of the branching fractions[1] $\mathcal{B}(B^0 \to D_s^{(*)+}D^{*-})$. We also report a measurement of the D_s^{*+} polarization in the decay $B^0 \to D_s^{*+}D^{*-}$, obtained from an angular analysis. These results provide tests of factorization with increased precision.

II. THE *BABAR* DETECTOR AND DATA SET

The data used in this analysis were collected with the *BABAR* detector at the PEP-II storage ring. An integrated luminosity of $20.8\,\mathrm{fb}^{-1}$ was recorded in 1999 and 2000 at the $\Upsilon(4S)$ resonance, corresponding to about 22.7 million produced $B\overline{B}$ pairs.

A detailed description of the *BABAR* detector is presented in Ref. [7]. Only the components of the detector most relevant to this analysis are briefly described here. Charged particles are reconstructed with a five-layer, double-sided silicon vertex tracker (SVT) and a 40-layer drift chamber (DCH) with a helium-based gas mixture, placed in a 1.5 T solenoidal field produced by a superconducting magnet. The charged particle resolution is approximately $(\delta p_T/p_T)^2 = (0.0013\,p_T)^2 + (0.0045)^2$, where p_T is the transverse momentum given in GeV/c. The SVT, with a typical single-hit resolution of $10\,\mu$m, provides measurement of the impact parameters of charged particle tracks in both the plane transverse to the beam direction and along the beam. Charged particle types are identified from the ionization energy loss ($\mathrm{d}E/\mathrm{d}x$) measured in the DCH and SVT, and the Cherenkov radiation detected in a ring imaging Cherenkov device (DIRC). Photons are identified by a CsI(Tl) electromagnetic calorimeter (EMC) with an energy resolution $\sigma(E)/E = 0.023 \cdot (E/\mathrm{GeV})^{-1/4} \oplus 0.019$.

III. METHOD OF PARTIAL RECONSTRUCTION

In selecting candidates for the decays $B^0 \to D_s^{(*)+}D^{*-}$ with $D^{*-} \to \overline{D}^0\pi^-$, no attempt is made to reconstruct the $\overline{D}^0$ decays. Only the $D_s^{(*)+}$ and the soft π^- from the D^{*-} decay are detected. In this way, the candidate selection efficiency is higher by almost an order of magnitude than that obtained with full reconstruction of the final state. Given the four-momenta of the $D_s^{(*)+}$ and π^-, and assuming they originate from a $B^0 \to D_s^{(*)+}D^{*-}$ decay, the four-momentum of the B^0 can be calculated up to an unknown azimuthal angle ϕ around the $D_s^{(*)+}$ flight direction. This calculation uses the constraint of the known center-of-mass (CM) energy and the masses of the B^0 and D^{*-} mesons. Energy and momentum conservation then allows a determination of the four-momentum of the $\overline{D}^0$, whose square yields the ϕ-dependent missing mass

$$M_{\mathrm{miss}} = \sqrt{(\mathrm{P}_B - \mathrm{P}_{D_s^{(*)+}} - \mathrm{P}_\pi)^2}\ , \qquad (1)$$

where P_B, $\mathrm{P}_{D_s^{(*)+}}$ and P_π are the four-momenta of the B^0, $D_s^{(*)+}$ and the soft pion, respectively. In this analysis the missing mass is defined with an arbitrary choice for the angle ϕ, such that the B^0 momentum $\mathbf{p}_B$ makes the smallest possible angle with $\mathbf{p}_\pi$ and $\mathbf{p}_{D_s^{(*)+}}$ in the CM frame.

IV. EVENT SELECTION

For each event, we calculate the ratio of the second to the zeroth order Fox-Wolfram moments, using all observed charged tracks and neutral clusters. This ratio is required to be less than 0.35 in order to suppress continuum $e^+e^- \to q\overline{q}$ events, where $q = u, d, s, c$.

We reconstruct D_s^+ mesons in the decay modes $D_s^+ \to \phi\pi^+$, $D_s^+ \to \overline{K}^{*0}K^+$ and $D_s^+ \to K_S^0K^+$, with subsequent decays $\phi \to K^+K^-$, $\overline{K}^{*0} \to K^-\pi^+$ and $K_S^0 \to \pi^+\pi^-$. These modes are selected since they offer the best combination of large branching fraction, good detection efficiency, and high signal-to-background ratio. Charged tracks from the D_s^+ are required to originate from within ± 10 cm along the beam direction and ± 1.5 cm in the transverse plane, and leave at least 12 hits in the DCH.

Kaons are identified using $\mathrm{d}E/\mathrm{d}x$ information from the SVT and DCH, as well as the Cherenkov angle and the number of photons measured with the DIRC. For each detector component $d = \{$SVT, DCH, DIRC$\}$, a likelihood L_d^K (L_d^π) is calculated given the kaon (pion) mass

[1] Reference to a specific decay channel or state also implies the charge conjugate decay or state. The notation $D_s^{(*)+}$ refers to either D_s^+ or D_s^{*+}.

hypothesis. A charged particle is classified as a "loose" kaon if it satisfies $L_d^K/L_d^\pi > 1$ for at least one of the detector components. A "tight" kaon classification is made if the condition $\prod_d L_d^K/L_d^\pi > 1$ is satisfied.

Three charged tracks consistent with originating from a common vertex are combined to form a D_s^+ candidate.

In the case of the decay $D_s^+ \to \phi\pi^+$, two oppositely charged tracks must be identified as kaons with both satisfying the loose criterion, and at least one, the tight criterion. No identification requirement is applied to the pion. The reconstructed invariant mass of the K^+K^- candidates must be within $8\,\mathrm{MeV}/c^2$ of the nominal ϕ mass [8]. In the decay $D_s^+ \to \phi\pi^+$, the ϕ meson is polarized longitudinally, resulting in the kaons having a $\cos^2\theta_H$ distribution, where θ_H is the angle between the K^+ and D_s^+ directions in the ϕ rest frame. We require $|\cos\theta_H| > 0.3$, which retains 97% of the signal while rejecting about 30% of the background.

In the reconstruction of the $D_s^+ \to \overline{K}^{*0}K^+$ mode, the $K^-\pi^+$ invariant mass is required to be within $65\,\mathrm{MeV}/c^2$ of the nominal $\overline{K}^{*0}$ mass [8]. This wider window leads to a larger fraction of combinatorial background than in the $D_s^+ \to \phi\pi^+$ mode. To reduce this background, we require $|\cos\theta_H| > 0.5$. In addition, substantial background arises from the decays $D^+ \to \overline{K}^{*0}\pi^+$ and $D^+ \to \overline{K}^0\pi^+$, which tend to peak around the nominal D_s^+ mass if the pion is misidentified as a kaon. This background is suppressed by requiring that the kaon daughter of the $\overline{K}^{*0}$ satisfy the loose kaon identification criterion and the other kaon, the tight criterion.

For the decay mode $D_s^+ \to K_S^0K^+$, with $K_S^0 \to \pi^+\pi^-$, the $\pi^+\pi^-$ invariant mass must be within $15\,\mathrm{MeV}/c^2$ of the nominal K_S^0 mass [8], and the charged kaon must satisfy the tight criterion. To improve the purity of the K_S^0 sample, we require the angle α between the K_S^0 momentum vector and the K_S^0 flight direction to satisfy $\cos\alpha > 0.98$.

The invariant mass M_{D_s} of D_s^+ candidates is required to be within three standard deviations (σ_{D_s}) of the signal distribution peak $M_{D_s}^{\mathrm{peak}}$ seen in the data.

D_s^+ candidates satisfying these selection criteria are combined with photon candidates to form $D_s^{*+} \to D_s^+\gamma$ candidates. Candidate photons are required to satisfy $E_\gamma > 50\,\mathrm{MeV}$, where E_γ is the photon energy in the laboratory frame, and $E_\gamma^* > 110\,\mathrm{MeV}$, where E_γ^* is the photon energy in the CM frame. When the photon candidate is combined with any other photon candidate in the event, the pair must not form a good π^0 candidate, defined by a total CM energy $E_{\gamma\gamma}^* > 200\,\mathrm{MeV}$ and an invariant mass $115 < M_{\gamma\gamma} < 155\,\mathrm{MeV}/c^2$.

The D_s^{*+} candidates must satisfy $|\Delta M - \Delta M^{\mathrm{peak}}| < 2.5\,\sigma_{\Delta M}$, where ΔM^{peak} is the peak of the signal $\Delta M = M(D_s^+\gamma) - M(D_s^+)$ distribution observed in the data. The CM momentum of the $D_s^{(*)+}$ candidate is required to be greater than $1.5\,\mathrm{GeV}/c$.

$D_s^{(*)+}$ candidates are combined with π^- candidates to form partially reconstructed $B^0 \to D_s^{(*)+}D^{*-}$ candidates. Since the transverse momentum of the pion in signal events is less than $210\,\mathrm{MeV}/c$, these tracks are not required to have DCH hits.

Due to the high combinatorial background in the ΔM distribution, more than one $D_s^{*+}\pi^-$ candidate pair is found per event, with about a 20% probability from signal Monte Carlo simulation. To select the best candidate in the event, the following χ^2 is calculated for each D_s^{*+} candidate

$$\chi^2 = \left[(M_i - M_i^{\mathrm{peak}})/\sigma_i\right]^2 + \left[(M_{D_s} - M_{D_s}^{\mathrm{peak}})/\sigma_{D_s}\right]^2 + \left[(\Delta M - \Delta M^{\mathrm{peak}})/\sigma_{\Delta M}\right]^2, \tag{2}$$

where M_i is the measured invariant mass of the intermediate $i = \phi$, K^{*0}, or K_S^0 candidate, depending on the D_s^+ decay mode, M_i^{peak} is the corresponding peak of the signal M_i distribution, and σ_i is its width obtained from data. The candidate with the smallest value of χ^2 in the event is retained.

V. RESULTS

The missing mass distributions of candidates for partially reconstructed $B^0 \to D_s^{(*)+}D^{*-}$ decays are shown in Fig. 1. A clear signal peak is observed in all modes. We perform a binned maximum likelihood fit to these distributions. The fit function is the sum of a Gaussian distribution and a background function given by

$$f_B(M_{\mathrm{miss}}) = \frac{C_1(M_0 - M_{\mathrm{miss}})^{C_2}}{C_3 + (M_0 - M_{\mathrm{miss}})^{C_2}}, \tag{3}$$

where C_i are parameters determined by the fit, and $M_0 \equiv M_{D^*} - M_\pi = 1.871\,\mathrm{GeV}/c^2$ is the kinematic end point. The fits find 3704 ± 232 and 1493 ± 95 events under the Gaussian peak in the sum of the $D_s^+\pi^-$ and $D_s^{*+}\pi^-$ distributions, respectively. However, due to the presence of cross feed and self-cross feed, discussed below, further analysis is needed in order to extract the signal yields and the branching fractions.

We use a Monte Carlo simulation, which includes both $B\overline{B}$ and $q\bar{q}$ continuum events, to study the missing mass distributions of the different background sources. We consider two kinds of backgrounds: a peaking component that contributes predominantly at the end of the missing mass distribution in the signal region and a non-peaking component that is more uniform. The non-peaking component is well modeled by the background function (3). The peaking component receives contributions from related channels due to

- **Cross Feed (CF):** if the soft photon from a $D_s^{*+} \to D_s^+\gamma$ decay is not reconstructed, $B^0 \to D_s^{*+}D^{*-}$ decays may lead to an enhancement under the signal peak of the $D_s^+\pi^-$ missing mass spectrum. Similarly, $B^0 \to D_s^+D^{*-}$ decays may lead to

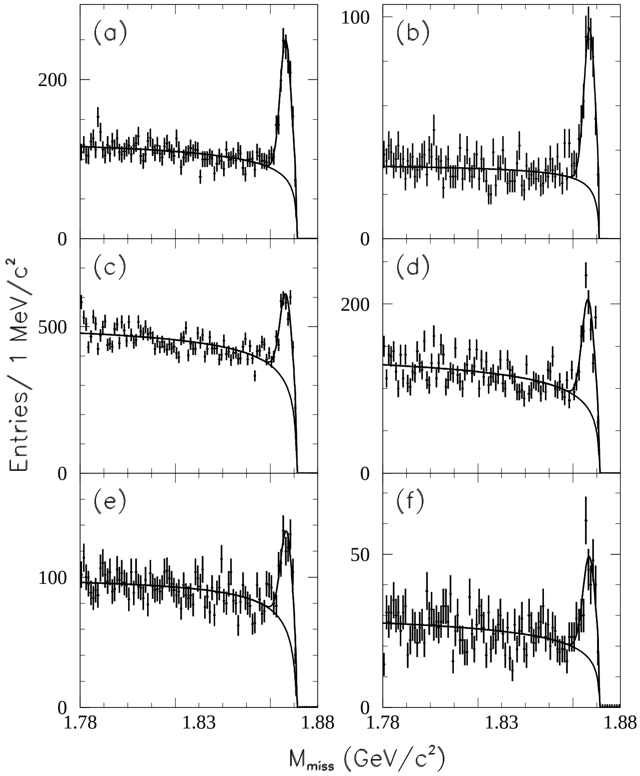

FIG. 1: Missing mass distributions of B candidates in data. (a) $D_s^+\pi^-$ with $D_s^+ \to \phi\pi^+$, (b) $D_s^{*+}\pi^-$ with $D_s^+ \to \phi\pi^+$, (c) $D_s^+\pi^-$ with $D_s^+ \to \overline{K}^{*0}K^+$, (d) $D_s^{*+}\pi^-$ with $D_s^+ \to \overline{K}^{*0}K^+$, (e) $D_s^+\pi^-$ with $D_s^+ \to K_S^0K^+$, (f) $D_s^{*+}\pi^-$ with $D_s^+ \to K_S^0K^+$. The curves show the result of the fit (see text), indicating the signal and background contributions.

a peaking enhancement in the $D_s^{*+}\pi^-$ $M_{\rm miss}$ spectrum, due to the combination of a D_s^+ with a random photon.

- **Self-Cross Feed (SCF):** this is due to true $B^0 \to D_s^{*+}D^{*-}$ decays in which the D_s^+ is correctly reconstructed, but combined with a random photon to produce the wrong D_s^{*+} candidate, resulting in a peaking enhancement in the $D_s^{*+}\pi^-$ spectrum.

Table I presents the reconstruction efficiency of correctly reconstructed signal $B^0 \to D_s^{(*)+}D^{*-}$ decays, as well as cross feed and self-cross feed, found for simulated events in the signal region $M_{\rm miss} > 1.86\,{\rm GeV}/c^2$.

In addition to these background sources, we also considered a possible contribution from the charged and neutral B decays $B \to D_s^{(*)+}\overline{D}^{**}$. These potential background sources were simulated with four $\overline{D}^{**}$ states: the observed $\overline{D}_1(2420)$ and $\overline{D}_2^*(2460)$ mesons, and the $\overline{D}_0^*(j=1/2)$ and $\overline{D}_1(j=1/2)$ mesons predicted by HQET [9]. Their contribution was determined to be negligible, mainly due to the $D_s^{(*)+}$ CM momentum cut.

TABLE I: Efficiencies for $B^0 \to D_s^{(*)+}D^{*-}$ decay modes to contribute to the $D_s^+\pi^-$ and $D_s^{*+}\pi^-$ missing mass distributions in the signal region $M_{\rm miss} > 1.86\,{\rm GeV}/c^2$. Two different $B^0 \to D_s^{*+}D^{*-}$ Monte Carlo samples have been used, one with longitudinal (long.) and the other with transverse (transv.) polarization.

	Reconstructed mode	
Generated mode	$D_s^+\pi^-$	$D_s^{*+}\pi^-$
$B^0 \to D_s^+D^{*-}$	$(23.6 \pm 1.0)\%$	$(1.7 \pm 0.3)\%$
$B^0 \to D_s^{*+}D^{*-}$ (long.)	$(9.0 \pm 0.3)\%$	$(7.4 \pm 0.3)\%$
Self-Cross Feed		$(1.6 \pm 0.1)\%$
$B^0 \to D_s^{*+}D^{*-}$ (transv.)	$(10.4 \pm 0.3)\%$	$(6.9 \pm 0.3)\%$
Self-Cross Feed		$(1.4 \pm 0.1)\%$

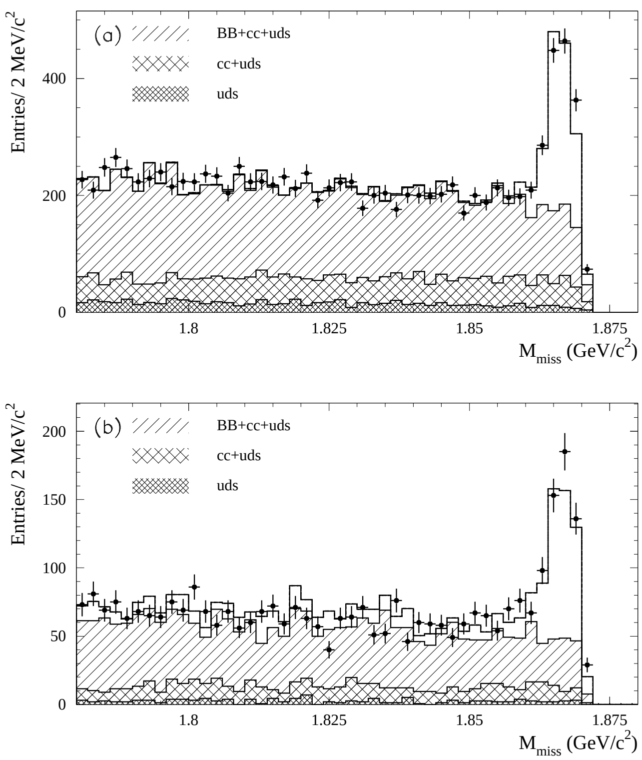

FIG. 2: Missing mass distribution for (a) $D_s^+\pi^-$ and (b) $D_s^{*+}\pi^-$ combinations for data (points with error bars) and Monte Carlo (histogram). The contributions from the $B\bar{B}$, $c\bar{c}$ and $q\bar{q}$ with $q = u,\ d,\ s$ (labeled *uds* in the figure) are shown separately. The cross feed and self-cross feed backgrounds are included in the total histogram, but not in the hatched $B\overline{B}$ histogram.

Multi-body decays $B \to D_s^{(*)+}X$ are found not to contribute due to the same cut.

Figure 2 shows a comparison of the missing mass distributions in data and Monte Carlo simulation. We assume 1.05% and 1.59% branching fractions for the $B^0 \to D_s^+D^{*-}$ and $B^0 \to D_s^{*+}D^{*-}$ decays, respectively, in the Monte Carlo simulation.

The number of events in the peaks in the $D_s^+\pi^-$ and $D_s^{*+}\pi^-$ $M_{\rm miss}$ distributions is obtained from the fits described above. The branching fractions are computed from these yields correcting for cross feed and self-cross feed background. This is done by inverting the 2×2 efficiency matrix, whose diagonal elements correspond to the sum of signal and self-cross feed efficiencies presented in Table I, and whose off-diagonal terms are the cross-feed efficiencies. The efficiencies corresponding to transverse and longitudinal polarization of $B^0 \to D_s^{*+}D^{*-}$ have been weighted according to the measured polarization discussed below. With this procedure, the $B^0 \to D_s^{(*)+}D^{*-}$ branching fractions are determined to be

$$\mathcal{B}(B^0 \to D_s^+ D^{*-}) = (1.03 \pm 0.14 \pm 0.13 \pm 0.26)\%, \quad (4)$$

$$\mathcal{B}(B^0 \to D_s^{*+} D^{*-}) = (1.97 \pm 0.15 \pm 0.30 \pm 0.49)\%, \quad (5)$$

and their sum is

$$\mathcal{B}(B^0 \to D_s^{(*)+} D^{*-}) = (3.00 \pm 0.19 \pm 0.39 \pm 0.75)\%, \quad (6)$$

where the first error is statistical, the second is the systematic error from all sources other than the uncertainty in the $D_s^+ \to \phi\pi^+$ branching fraction, and the third error, which is dominant, is due the uncertainty in the $D_s^+ \to \phi\pi^+$ branching fraction $\mathcal{B}(D_s^+ \to \phi\pi^+) = (3.6 \pm 0.9)\%$ [8]. Correlations in the systematic errors between Eqs. (4) and (5) are taken into account in Eq. (6). The sources of the systematic error are discussed in Sec. VI.

The measurement of the fraction of the longitudinal polarization Γ_L/Γ in the $B^0 \to D_s^{*+}D^{*-}$ decay mode is performed for candidates having missing mass in the signal region ($M_{miss} > 1.86\,{\rm GeV}/c^2$). To minimize the systematic error due to large backgrounds, the polarization measurement involves only the $D_s^+ \to \phi\pi^+$ channel, which has the best signal to background ratio. Two angles are used: the helicity angle θ_γ between the D^{*-} and the soft photon direction in the D_s^{*+} rest frame, and the helicity angle θ_π between the D_s^{*+} and the soft pion direction in the D^{*-} rest frame. Since the B meson is not fully reconstructed, we compute θ_γ and θ_π by constraining $M_{\rm miss}$ to the nominal D^0 mass [8] to obtain a unique solution for the azimuth ϕ.

The two-dimensional distribution ($\cos\theta_\gamma$, $\cos\theta_\pi$) is divided into five ranges in each dimension, resulting in 25 bins. The combinatorial background, as well as the cross feed and the self-cross feed obtained from Monte Carlo simulation, are subtracted from this two-dimensional data distribution. The resulting signal distribution is corrected bin-by-bin for detection efficiency, which is obtained from the simulation separately for each bin. A two-dimensional binned minimum-χ^2 fit is then performed to the efficiency-corrected signal distribution with the fit function

$$\frac{d^2\Gamma}{d\cos\theta_\pi \, d\cos\theta_\gamma} \propto \frac{\Gamma_L}{\Gamma} \cos^2\theta_\pi \sin^2\theta_\gamma + \left(1 - \frac{\Gamma_L}{\Gamma}\right)\sin^2\theta_\pi \frac{1+\cos^2\theta_\gamma}{4}. \quad (7)$$

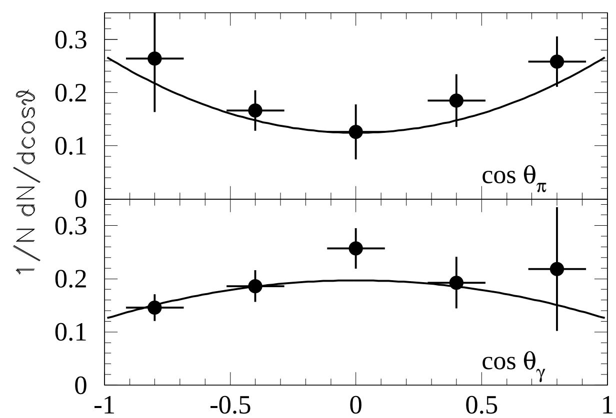

FIG. 3: Projections of the number of background-subtracted data events on the $\cos\theta_\pi$ and $\cos\theta_\gamma$ axes. The result of the two-dimensional fit is overlaid.

The resulting fit has a χ^2 of 23.1 for 25 bins with two floating parameters (Γ_L/Γ and total normalization). Figure 3 shows the data and the result of the fit projected on the $\cos\theta_\gamma$ and $\cos\theta_\pi$ axes.

From the fit, the fraction of longitudinal polarization is determined to be

$$\Gamma_L/\Gamma = (51.9 \pm 5.0 \pm 2.8)\%, \quad (8)$$

where the first error is statistical and the second is systematic.

VI. SYSTEMATIC UNCERTAINTIES

The various contributions to the systematic errors on the branching fraction and polarization measurements are summarized in Table II. The dominant systematic error for the branching fractions is the uncertainty on the three D_s^+ branching fractions. To evaluate the uncertainty due to the background subtraction, the signal yield is determined using an alternative method in which the number of events is extracted directly from the histogram after subtraction of the background, which is estimated with the Monte Carlo simulation. The difference of the signal yields obtained in this way from the results of the fit was taken as a systematic error. This also accounts for the systematic error due to a possible deviation of the signal shape from a Gaussian.

The Monte Carlo statistical errors in the determination of the signal and the cross feed efficiencies are included as a systematic error. The uncertainty in the calculation of the $B^0 \to D_s^{*+}D^{*-}$ polarization is propagated to the branching fraction systematic error. The systematic error due to the uncertainty on the efficiency for the reconstruction of charged particles is 1.2% times the number of charged particles in the decay. An additional error of 1.6% is added in quadrature to account for the uncertainty in the reconstruction efficiency of the soft pion.

TABLE II: Sources of systematic uncertainties (%) for the $B^0 \to D_s^{(*)+} D^{*-}$ branching fractions and $B^0 \to D_s^{*+} D^{*-}$ polarization measurements.

Source	$D_s^+ D^{*-}$	$D_s^{*+} D^{*-}$	$\sigma(\Gamma_L/\Gamma)$
Background subtraction or modeling	2.7	5.9	0.5
Monte Carlo statistics	4.2	6.0	2.7
Polarization uncertainty	0.8	0.5	-
Cross feed	3.2	2.4	-
Number of B pairs	1.6	1.6	-
$\mathcal{B}(\phi \to K^+K^-)$	1.6	1.6	-
Particle identification	1.0	1.0	0.1
Tracking efficiency	3.6	3.6	0.5
Soft pion efficiency	2.0	2.0	0.2
Relative branching fractions	10.2	10.2	-
$\mathcal{B}(D_s^{*+} \to D_s^+\gamma)$	-	2.7	-
Photon efficiency	-	1.3	0.1
π^0 veto	-	2.7	0.3
Total systematic error	13.1	15.1	2.8

The systematic error due to the π^0 veto requirement was studied by measuring the relative D_s^{*+} yields in data and Monte Carlo with and without the π^0 veto.

In the polarization measurement, the level of the various backgrounds depends on the charged track, neutral cluster, and particle identification efficiencies. The fit was repeated varying the background according to the errors in these efficiencies, and the resulting variations in Γ_L/Γ were taken as the associated systematic error.

TABLE III: The fractional difference $\langle (N_{\rm D} - N_{\rm MC})/N_{\rm MC}\rangle$, averaged over all $M_{\rm miss}$ bins, where $N_{\rm D}$ ($N_{\rm MC}$) is the number of data (Monte Carlo) candidates in a given bin of the $M_{\rm miss}$ distribution of the given control sample. SB (SR) refers to the M_{D_s} or ΔM sideband (signal region) control sample. WS indicates wrong sign $D_s^{(*)+}\pi^+$ combinations, and $-p^*_{D_s^{(*)+}}$ indicates that $M_{\rm miss}$ was calculated from the negative of the $D_s^{(*)+}$ CM momentum. The missing mass range $1.78 < M_{\rm miss} < 1.87\,{\rm GeV}/c^2$ is used for the control sample, except for the first line.

Sample type	$D_s^+\pi^-$	$D_s^{*+}\pi^-$
$1.78 < M_{\rm miss} < 1.85\,{\rm GeV}/c^2$	-0.009 ± 0.007	0.075 ± 0.014
SB	-0.075 ± 0.006	0.007 ± 0.022
SR, WS	0.006 ± 0.008	0.044 ± 0.015
SB, WS	-0.060 ± 0.007	-0.008 ± 0.024
SR, $-p^*_{D_s^{(*)+}}$	0.015 ± 0.009	0.075 ± 0.016
SB, $-p^*_{D_s^{(*)+}}$	-0.062 ± 0.007	-0.123 ± 0.022
Average	-0.038 ± 0.003	0.032 ± 0.007

To check that the simulation accurately reproduces the background $M_{\rm miss}$ distributions in the data, a thorough data-Monte Carlo comparison is made in control samples containing no signal events. These samples are events with $1.78 < M_{\rm miss} < 1.85\,{\rm GeV}/c^2$; events in the D_s^+ sideband $1.89 < M_{D_s} < 1.95\,{\rm GeV}/c^2$ or $1.985 < M_{D_s} < 2.05\,{\rm GeV}/c^2$; events in the D_s^{*+} sideband $170 < \Delta M < 300\,{\rm MeV}/c^2$; wrong sign $D_s^{(*)+}\pi^+$ combinations in either the M_{D_s} and ΔM sidebands or signal regions determined above; and candidates in which $M_{\rm miss}$ was calculated with the inverse of the $D_s^{(*)+}$ center-of-mass momentum $p^*_{D_s^{(*)+}}$. The comparison between data and Monte Carlo simulation for these control samples is shown in Table III. The average level of discrepancy is used to estimate the uncertainty in the modeling of the background.

VII. SUMMARY

In summary, based on a partial reconstruction technique, we have measured the branching fractions

$$\begin{aligned}
\mathcal{B}(B^0 \to D_s^+ D^{*-}) &= (1.03 \pm 0.14 \pm 0.13 \pm 0.26)\%\ ,\\
\mathcal{B}(B^0 \to D_s^{*+} D^{*-}) &= (1.97 \pm 0.15 \pm 0.30 \pm 0.49)\%\ ,\\
\mathcal{B}(B^0 \to D_s^{(*)+} D^{*-}) &= (3.00 \pm 0.19 \pm 0.39 \pm 0.75)\%\ .
\end{aligned}$$

The fraction of the longitudinal D_s^{*+} polarization in $B^0 \to D_s^{*+} D^{*-}$ decays is determined to be

$$\Gamma_L/\Gamma = (51.9 \pm 5.0 \pm 2.8)\%.$$

This measurement is consistent with theoretical predictions assuming factorization, which range from 50 to 55% [10, 11]. Our results are also in good agreement with previous experimental results [3, 6].

VIII. ACKNOWLEDGMENTS

We are grateful for the excellent luminosity and machine conditions provided by our PEP-II colleagues, and for the substantial dedicated effort from the computing organizations that support *BABAR*. The collaborating institutions wish to thank SLAC for its support and kind hospitality. This work is supported by DOE and NSF (USA), NSERC (Canada), IHEP (China), CEA and CNRS-IN2P3 (France), BMBF and DFG (Germany), INFN (Italy), NFR (Norway), MIST (Russia), and PPARC (United Kingdom). Individuals have received support from the A. P. Sloan Foundation, Research Corporation, and Alexander von Humboldt Foundation.

[1] M. Bauer, B. Stech, M. Wirbel, Z. Phys. C **34**, 103 (1987).
[2] CLEO Collaboration, M. S. Alam *et al.*, Phys. Rev. D **50**, 43 (1994).
[3] CLEO Collaboration, D. Gibaut *et al.*, Phys. Rev. D **53**, 4734 (1996).
[4] CLEO Collaboration, G. Bonvicini *et al.*, CLEO CONF 98-23, presented at the 29^{th} International Conference on High Energy Physics, Vancouver, Canada (1998).
[5] CLEO Collaboration, J. P. Alexander *et al.*, Phys. Rev. D **64**, 092001 (2001).
[6] CLEO Collaboration, S. Ahmed *et al.*, Phys. Rev. D **62**, 112003 (2000).
[7] *BABAR* Collaboration, A. Palano *et al.*, Nucl. Instr. Meth. A **479**, 1 (2002).
[8] Particle Data Group, K. Hagiwara *et al.*, Phys. Rev. D **66**, 010001 (2002).
[9] A. F. Falk and M. Luke, Phys. Lett. B **292**, 119 (1992).
[10] J. D. Richman, in *Probing the Standard Model of Particle Interactions*, edited by R. Gupta, A. Morel, E. de Rafael, and F. David (Elsevier, Amsterdam, 1999), p.640.
[11] Z. Luo and J. L. Rosner, Phys. Rev. D **64**, 094001 (2001).